

Far Ultraviolet Observations of the Dwarf Nova VW Hyi in Quiescence ¹

Patrick Godon², Edward M. Sion

*Astronomy and Astrophysics, Villanova University,
800 Lancaster Avenue, Villanova, PA 19085, USA*

patrick.godon@villanova.edu edward.sion@villanova.edu

F. H. Cheng

*Department of Physics, Shanghai University, 99 Shang-Da Road, Shanghai 200436, P.R.
China*

cheng3@prodigy.net

Paula Szkody

Department of Astronomy, University of Washington, Seattle, WA 98195, USA

szkody@alica.astro.washington.edu

Knox S. Long

Space Telescope Science Institute, 3700 San Martin Drive, Baltimore, MD 21218, USA

long@stsci.edu

Cynthia S. Froning

*Center for Astrophysics and Space Astronomy, University of Colorado, 593 UCB, Boulder,
CO 80309, USA*

cfroning@casa.colorado.edu

ABSTRACT

We present a 904-1183 Å spectrum of the dwarf nova VW Hydri taken with the *Far Ultraviolet Spectroscopic Explorer* during quiescence, eleven days after

²Visiting at the Space Telescope Science Institute, Baltimore, MD 21218, USA

a normal outburst, when the underlying white dwarf accreter is clearly exposed in the far ultraviolet. However, model fitting show that a uniform temperature white dwarf does not reproduce the overall spectrum, especially at the shortest wavelengths. A better approximation to the spectrum is obtained with a model consisting of a white dwarf and a rapidly rotating “accretion belt”. The white dwarf component accounts for 83% of the total flux, has a temperature of 23,000K, a $v \sin i = 400 \text{ km s}^{-1}$, and a low carbon abundance. The best-fit accretion belt component accounts for 17% of the total flux, has a temperature of about 48,000 – 50,000K, and a rotation rate $V_{rot} \sin i$ around 3,000 – 4,000 km s^{-1} . The requirement of two components in the modeling of the spectrum of VW Hyi in quiescence helps to resolve some of the differences in interpretation of ultraviolet spectra of VW Hyi in quiescence. However, the physical existence of a second component (and its exact nature) in VW Hyi itself is still relatively uncertain, given the lack of better models for spectra of the inner disk in a quiescent dwarf nova.

Subject headings: accretion, accretion disks - novae, cataclysmic variables - stars: dwarf novae - stars: individual (VW Hydri) - white dwarfs

1. Introduction: Accretion Onto White Dwarfs in Dwarf Novae

1.1. Dwarf Novae

Dwarf novae (DNe) are a subclass of cataclysmic variable (CV) systems, in which a white dwarf (WD, the primary) accretes hydrogen-rich matter from a low-mass main sequence-like star (the secondary) filling its Roche lobe. In these systems, the transferred gas forms an accretion disk around the WD. It is believed that the accretion disk is subject to a thermal instability that causes cyclic changes of the accretion rate. A low rate of accretion ($\approx 10^{-11} M_{\odot} \text{ yr}^{-1}$) quiescent stage is followed every few weeks to months by a high rate of accretion ($\approx 10^{-8} M_{\odot} \text{ yr}^{-1}$) outburst stage of days to weeks. These outbursts (dwarf nova - DN accretion event or nova-like high state), are believed to be punctuated every few thousand years or more by a thermonuclear runaway (TNR) explosion: the classical nova (Hack & la Dous 1993).

¹Based on observations made with the NASA-CNES-CSA *Far Ultraviolet Spectroscopic Explorer*. *FUSE* is operated for NASA by the Johns Hopkins University under NASA contract NAS5-32985

The WD dominates the far ultraviolet (FUV) in many, and probably, most, DNe in quiescence. As a consequence, quiescent DNe provide a unique laboratory not only for understanding the physics of accretion but also for understanding physical processes of WDs. As a result, *Hubble Space Telescope* (*HST*) and other UV observatories have been used to directly observe the effects of accretion on the WDs of these systems. These studies have yielded determinations of effective temperature, the rotation rates, photospheric abundances, cooling rates following outburst, and dynamical masses in a number of DNe (Sion 1999; Gänsicke 1999).

However, there are some indications of an additional component besides the white dwarf in the spectra of some DNe in quiescence, such as the presence of emission lines and the bottoms of Lyman alpha profiles which do not go to zero as in a pure white dwarf. Possible locations of this additional component could be: (1) a heated region of the WD; (2) direct emission from the boundary layer; (3) an optically thick region of the disk; or (4) a corona/chromosphere above a cool disk (Ko & Kallman 1989, 1992; Meyer & Meyer-Hofmeister 1989; Ko et al. 1996; Liu, Meyer & Meier-Hofmeister 1997; La Dous, Meyer, & Meyer-Hofmeister 1997).

1.2. VW Hyi

VW Hyi is a key system for understanding DNe in general. It is the closest (Warner 1987, placed it at 65 pc) and brightest example of an SU UMa-type DN and it lies along a line of sight with an exceptionally low interstellar column (Polidan, Mauche & Wade 1990, estimated the HI column to be $\approx 6 \times 10^{17} \text{ cm}^{-2}$), which has permitted study of VW Hyi in nearly all wavelength ranges, including detection in the usual opaque extreme ultraviolet [EUVE (Mauche 1996)]. For these reasons, it is one of the best-studied systems. Coherent and quasi-coherent soft X-ray oscillations and a surprisingly low luminosity boundary layer (BL) have been detected (Belloni et al. 1991; Mauche et al. 1991). VW Hyi is below the CV period gap near its lower edge, with an orbital period of 107 minutes and a quiescent optical magnitude of 13.8. It is a member of the SU UMa class of DNe, which undergo both normal DN outbursts and superoutbursts. The normal outbursts last 1-3 days and occur every 20-30 days, with peak visual magnitude of 9.5. The superoutbursts last 10-15 days and occur every 5-6 months, with peak visual magnitude reaching 8.5. The mass of the accreting WD was estimated to be $0.63 M_{\odot}$ (Schoembs & Vogt 1981), but more recently a gravitational redshift determination yielded a larger mass $M_{wd} = 0.86 M_{\odot}$ (Sion et al. 1997). Below the period gap, gravitational wave emission is thought to drive mass transfer, resulting in very low accretion rates during dwarf nova quiescence. The inclination of the

system is ≈ 60 degrees (Huang et al. 1996a,b).

VW Hyi was first observed at FUV wavelengths with *IUE*. Based on observations of VW Hyi in quiescence, which showed a broad absorption profile centered on Lyman α , Mateo & Szkody (1984) argued that FUV light from the system was dominated by the WD with $T_{eff} = 18,000 \pm 2,000$ K (for $\log g=8$). Much higher S/N spectra were obtained with *HST*. In particular, Sion et al. (1995, 1996, 2001) confirmed the basic shape of the spectrum and concluded that the temperature of the WD varied by at least 2,000 K depending on the time since outburst. They also presented evidence for CNO processing of material in the WD photosphere from the relatively narrow metal lines in the spectrum, as well as for a rapidly rotating “accretion belt” in the system. The accretion belt was to be understood physically as a region of the WD surface spun up by accreting material with Keplerian velocities. Furthermore, Sion et al. (1997), using the GHRS on *HST*, measured the gravitational redshift of the WD and concluded that the mass of the WD was $0.86^{+0.18}_{-0.32} M_{\odot}$ and that the rotation rate of the WD was ~ 400 km s $^{-1}$. All of these observation were limited to a wavelength range longward of about 1150 Å. However, an 820-1840 Å spectrum of VW Hyi was obtained using the Hopkins Ultraviolet Telescope (HUT). Long et al. (1996) found that the HUT spectrum was reasonably consistent with a WD with a temperature of about 17,000K, but that an improved fit to the data at that time could be obtained with a combination of emission from a WD and an accretion disk.

Long et al. (1996) suggested that higher S/N spectra of VW Hyi in quiescence are “needed to unambiguously assess the disk contribution to the FUV spectrum of VW Hyi in quiescence”. Here we have attempted to follow-up on that suggestion by observing VW Hyi in quiescence with the *Far Ultraviolet Spectroscopic Explorer (FUSE)*. With a practical wavelength range of 904-1188 Å, FUSE is sensitive to a second component, since the expected flux from a WD with a temperature of about 20,000 K is very different at 950 and 1100 Å. In addition, the *FUSE* spectral range and high spectral resolution allows the study of a broad range of line transitions.

The remainder of the paper is organized as follows. In Section 2, we describe the observations and provide a description of the spectra that were obtained. In Section 3, we compare the spectrum to models in an attempt to decompose the spectrum into its constituent parts. In Section 4, we discuss the origin of the second component in the spectrum, and in Section 5, we briefly summarize our conclusions.

2. Observations and Data Reduction

2.1. The Observations

FUSE is a low-earth orbit satellite, launched in June 1999 (Moos et al. 2000). Its optical system consists of four optical telescopes (mirrors), each separately connected to a different Rowland spectrograph. The 4 diffraction gratings of the 4 Rowland spectrographs produce 4 independent spectra on two photon counting area detectors. The total spectral wavelength coverage extends from 904 Å to 1188 Å with a resolution of $R \approx 12000$. Two mirrors and two gratings are coated with SiC to provide wavelength coverage below 1020 Å, while the other two mirrors and gratings are coated with Al and a LiF overcoat. The Al+LiF coating provides about twice the reflectivity of SiC at wavelengths > 1050 Å, and very little reflectivity below 1020 Å (hereafter the SiC1, SiC2, LiF1 and LiF2 channels). The observatory, its operations, and performance have been described in detail by Sahnou et al. (2000).

The *FUSE* observation of VW Hyi occurred on August 29th, 2001 at 16:48 UT (JD2452151) approximately 11 days after the last outburst. The overall exposure time was 18,004 seconds through the LWRS aperture, acquired in 9 exposures ranging from $\simeq 600$ to 3500 seconds each. The data were obtained in time-tag mode. Of the 9 exposures acquired, all but the first two experienced a series of event bursts (Sahnou et al. 2000) that were strongest in segments LiF1A and LiF1B but affected all eight segment spectra. We re-processed the data using V.2.1.6 of the CALFUSE pipeline, which includes screening and removal of event bursts during data reduction. We combined the resulting exposures and data segments to create a time-averaged spectrum with a linear, 0.1 Å dispersion, weighting the flux in each output datum by the exposure time and sensitivity of the input exposure and channel of origin. The S/N is about 10:1 at a resolution of 0.1 Å. Due to the “worm”, the data in the LiF1 channel longward of ≈ 1130 Å were removed. Because of that, the practical spectral range of *FUSE* was reduced to 905-1182 Å.

2.2. The Spectrum

In Figure 1, the *FUSE* spectrum is displayed in a flux versus wavelength plot with the principal line features labeled with tick marks. An interesting aspect of the spectrum is that while the region longward of 1010 Å shows features that can clearly be identified as absorption lines, the region shortward of this does not. The most obvious absorption lines are NII (1085.7 Å), SiIII (at 1113.2, 1144.3, and 1160.2 Å) and the (familiar) CIII (1174.9-1176.4 Å). In table 1, the line measurements (equivalent widths, full widths at half-maximum, ion

identifications and wavelengths) are presented. In addition, there is an emission feature redward of Lyman β , at 1033 Å and 1037 Å, that we identify as OVI emission lines.

We note that the flux level of the *FUSE* spectrum, in the range of wavelength overlap with STIS E140M spectra (i.e. around 1150-1182 Å), matches rather closely (within about 10%) the HST flux value of $\approx 2 \times 10^{-13}$ erg s $^{-1}$ cm $^{-2}$ Å $^{-1}$. And a comparison of the *FUSE* spectrum to that obtained with HUT (Long et al. 1996) indicates (a) that the overall spectral shape appears rather similar, but (b) that the *FUSE* spectrum clearly shows emission extending to the Lyman limit. There is clearly a rise in the flux in the region of the Lyman limit.

2.3. Variability

We also examined the variability among the 9 exposures in the observations by calculating the standard deviation about the mean flux in three wavelength regions: 917 – 936 Å, 953 – 970 Å, and 1050 – 1070 Å. These three regions sample the spectrum at the short wavelength emission peak, slightly longward of the emission peak, and to the red of Lyman beta. In a single channel (SiC2), the standard deviation about the mean for the 9 exposures was 21%, 15%, and 8%, respectively, indicating that the FUV spectrum of VW Hyi does fluctuate, with the variability strongest at the shortest wavelengths, where the WD does not contribute.

3. Analysis

In this section we describe the procedure we follow to assess the temperature, rotation rate and chemical abundances of the accreting WD in VW Hyi. This procedure consists of comparing the observed *FUSE* spectrum of VW Hyi with a grid of theoretical spectra obtained assuming different assumptions and for different values of the parameters of the system as explained below. For this purpose, we use a combination of synthetic stellar, disk and accretion belt spectra. The best fit models are then obtained using a χ^2 minimization fitting procedure.

The stellar atmosphere models and the accretion belt models are both generated using the TLUSTY code (Hubeny 1988) for different values of the parameters of the accreting WD, such as temperature, composition and surface gravity. A spectrum synthesis code (SYNSPEC) is then used to generate the spectra of the stellar atmospheres obtained in TLUSTY (Hubeny et al. 1994; Hubeny & Lanz 1995).

For the accretion disk spectrum, we used the grid of accretion disk spectra computed by Wade & Hubeny (1998), who use a slightly different version of the TLUSTY code (TLUSDISK) to generate the theoretical spectrum of an accretion disk. The accretion disk model is really made of a collection of rings. The disk models are computed assuming LTE and vertical hydrostatic equilibrium. Irradiation from external sources is neglected. Local spectra of disk annuli are computed taking into account line transition from elements 1-28 (H through Ni). Limb darkening as well as Doppler broadening and blending of lines are taken into account.

Then, to carry out the model fits, we masked the following wavelength regions where several narrow emission-like features occur in the *FUSE* spectrum: [948-952Å], [972-974Å], [989-993Å], [1025-1041Å], [1078-1082Å], [1092-1096Å], [1168-1170Å]. Most of these emission lines are due to air glow, when part of the observations are carried out during day time. In particular we masked the OVI emission lines around 1033 Å and 1037 Å.

Details of the codes and the χ^2_ν (χ^2 per degree of freedom) minimization fitting procedures are discussed in detail in Sion et al. (1995) and Huang et al. (1996a), and will not be repeated here.

3.1. The white dwarf model

We took the WD photospheric temperature T_{eff} , $\log g$, Si and C abundances, and rotational velocity $V_{rot} \sin i$ as free parameters. Since our WD model spectra are normalized to 1 solar radius at a distance of 1 kiloparsec, the distance d of a source is related to the scale factor S :

$$d = 1000(pc) \times (R_{wd}/R_\odot)/\sqrt{S},$$

and the scale factor S is the factor by which the theoretical fluxes have to be multiplied in order to fit the observed fluxes. In the first model presented here we fixed $d = 65$ pc while the radius (and consequently the mass) of the WD was allowed to change. However, other models presented here have been computed assuming a fixed radius (corresponding to $M_{wd} = 0.86M_\odot$).

The grid of models for the one component (white dwarf only) extended over the following range of parameters: $T_{wd}/1000K = 22, 23, \dots, 36$; Si = 0.1, 0.2, 0.5, 1.0, 2.0, 5.0 (times solar); C = 0.1, 0.2, 0.5, 1.0, 2.0, 5.0 (times solar); $V_{rot} \sin i = 100, 200, 400, 600, 800$ km s⁻¹; and $\log g = 7.5$ to 9.0 by increment of 0.1.

For the single temperature white dwarf models, we found the best-fitting results with 3-sigma error bars to be $T_{wd}/1000(K) = 26.0 + 0.2/-0.4$, Si abundance = $0.5 + 0.3/-0.1 \times$ solar,

C abundance = $0.1 + 0.2/-0.1 \times$ solar, $\log g = 8.8$ and $V_{rot} \sin i = 400 + 100/-200$ km s⁻¹. This best-fit has a $\chi^2_\nu = 14.81$ with a mass of $M_{wd} = 1.14M_\odot$. The best single-temperature white dwarf model fit is displayed in figure 2 (see also Table 2: model 1).

Following the suggestion of an anonymous referee, we also modified our fitting code to keep both the distance (65 pc) and the radius (7×10^8 cm for a $0.86M_\odot$, or equivalently $\log g = 8.37$) fixed at the same time. These parameters defined a single value of the scale factor S . In this way, we proceeded to find the best fitting models by varying the temperature and composition while keeping $\log g$ fixed.

In Table 2 we present 4 WD models (models # 2, 3, 4, & 5) with a fixed $\log g = 8.37$ and a fixed distance of 65 pc. The best model has a $T = 22,000$ K, and a $\chi^2_\nu = 28.2$. Here we have assumed solar abundances. Changing the abundances modestly improves the χ^2_ν value.

Thus an interesting comparison became possible with our original fitting procedure where the scale factor was variable. In the case of the WD only, the fixed scale factor models do not improve the fit, and the best fit model has a χ^2_ν value twice as large as the one obtained when allowing S to vary. We used the same masked regions as we did in the variable scale factor fitting. We should note, however, that while we assumed $M = 0.86M_\odot$, the mass estimate from Sion et al. (1997) of $0.86M_\odot$ has an error bar of $^{+0.18}_{-0.32}M_\odot$. This makes the mass and the radius of the WD known within a factor of 2: $0.54 < M_{wd}/M_\odot < 1.04$ with a WD radius corresponding to $6,000\text{km} < R_{wd} < 12,000\text{km}$, or equivalently $7.5 < \log g < 8.56$, which justifies our original fitting procedure where we kept $\log g$ and consequently M_{wd} and R_{wd} as free parameters.

3.2. The accretion disk model

Due to the relatively poor fit using single temperature WD models, particularly the flux deficit of the model at short wavelengths, we explored whether an accretion disk model would produce better agreement with the *FUSE* spectrum. Although one expects the inner region of the accretion disk in VW Hyi to be optically thin during quiescence, the lack of such models led us to consider how well optically thick steady state disks can represent the *FUSE* observation.

In the present work we used the grid of accretion disk spectra of Wade & Hubeny (1998) consisting of 26 different combinations of M_{wd} (0.35, 0.55, 0.80, 1.03 and $1.21 M_\odot$) and \dot{M} ($\log \dot{M} = -8.0, -8.5, -9.0, -9.5, -10.0$ and $-10.5 \dot{M} \text{ yr}^{-1}$; see Table 2 in Wade & Hubeny (1998)) and the spectra are presented for six different disk inclinations i (8.1, 18.2, 41.4, 60.0, 75.5 and 81.4 degrees), in the form of nonprojected flux (however, the projection of the Keplerian

velocities is included) scaled to a distance of 100 pc. Here, we corrected for the projected flux and the distance is related to scale factor:

$$d = 100(pc)/\sqrt{S}.$$

First, we fixed only the distance $d=65$ pc and kept M_{wd} as a free parameter. The best-fitting accretion disk model (model # 6 in Table 2) corresponded to $M_{wd} = 1.03M_{\odot}$, $\dot{M} = 1 \times 10^{-10.5}M_{\odot}/\text{yr}^{-1}$, inclination angle $i = 81$ degrees. With a χ^2_{ν} value of 19.9, this disk only fit is significantly worse than the single-temperature white dwarf fit (see figure 3). This should not be surprising since the white dwarf is the dominant FUV emitter in the system (Mateo & Szkody 1984; Sion et al. 1995, 1996, 1997, 2001; Long et al. 1996).

Next, we fixed the distance $d=65$ pc and chose $M = 0.8M_{\odot}$ (in better agreement with the mass estimate of $0.86M_{\odot}$). The best-fitting accretion disk model (model # 8 in Table 2) corresponded to $\dot{M} = 1 \times 10^{-10}M_{\odot}/\text{yr}^{-1}$, inclination angle $i = 60$ degrees with a χ^2_{ν} value of 29.83. In Table 2 we present 2 additional models (7 & 9 in Table 2), one with a higher accretion rate and one with a lower accretion rate, to emphasize how drastically the χ^2_{ν} value can worsen from one model to another when changing the accretion rate.

3.3. Composite model: WD plus accretion disk

Next we tried a combination of a WD plus an optically thick disk. We created a grid in WD temperature T_{eff} from 16,000K to 35,000K in steps of 1000K, with each time a mass M_{wd} in agreement with a white dwarf mass the same as each one assumed in the grid of disk models of Wade & Hubeny (1998). The disk flux is divided by 100 to normalize it at 1000pc to match the WD flux, then both fluxes are added for comparison with the observed flux. In that cases one has:

$$F_{obs} = [F_{wd} (R_{wd}/R_{\odot})^2 + F_{disk}/100] \times S;$$

where F_{obs} is the observed FUSE flux (integrated over the entire FUSE wavelength range), F_{wd} is the theoretical (integrated) flux of the WD, F_{disk} is the theoretical (integrated) flux of the disk, and $d = 1000/\sqrt{S}$ pc.

Here too, we started by fixing $d = 65$ pc. The best-fitting disk plus WD combination, yielded $T_{eff} = 23,000K$, $V_{rot} \sin i = 400\text{km s}^{-1}$, $\text{Si} = 0.5 \times \text{solar}$, $\text{C} = 0.1 \times \text{solar}$, $M_{wd} = 1.21M_{\odot}$, with a disk model having an accretion rate $10^{-10.5}M_{\odot}/\text{yr}^{-1}$ and $i = 81$ degrees. The combination fit had a $\chi^2_{\nu} = 11.03$. In this fit, the WD contributed 64% of the flux and the accretion disk 36% of the flux. This composite model is shown in Figure 4 and is listed in Table 2 (model 10).

We then tried a model in which we fixed both $d=65\text{pc}$ and the radius R_{wd} of the WD. The disk models (from the grid of models of Wade & Hubeny (1998)) with parameters in best agreement with the parameters of the VW Hyi systems are the disk models with $M_{wd} = 0.8M_{\odot}$ (corresponding to $\log g = 8.23$) and $i = 60$ degrees. The best such composite WD plus disk fit model is presented in Table 2 (model 11), with $T_{wd} = 21,000\text{K}$, $\dot{M} = 10^{-10.5}M_{\odot}\text{yr}^{-1}$, $V_{rot} \sin i = 400\text{km s}^{-1}$ with a $\chi^2_{\nu} = 32.9$. Here too we assumed solar abundances for simplicity. The WD contributes 88% of the flux while the disk contributes 12% of the flux.

3.4. Composite model: WD plus accretion belt

Lastly, we tried a combination of a WD plus an accretion belt. The accretion belt model is really a stellar atmosphere model but with only a fractional area of the WD and parameters consistent with a fast rotating hot accretion belt. Since the belt is fast rotating its effective gravity is reduced to a fraction of the gravity of the star as follows:

$$g_{belt} = g_{wd} - \frac{V_{belt}^2}{R_{wd}}.$$

Once $\log g_{wd}$ is set, there is a direct relation between the gravity of the belt $\log g_{belt}$ and its velocity V_{belt} . For the accretion belt plus WD composite models, we created a grid in WD temperature T_{eff} from 16,000K to 35,000K in steps of 1000K, and in accretion belt temperature T_{belt} from 25,000K to 55,000K in steps of 1000K. However, the results are not very sensitive to the value of $\log g_{belt}$ as long as $\log g_{belt} < 7.5$, corresponding to $V_{belt} \sin i \approx 3,000 - 4,000 \text{ km s}^{-1}$, where the lower limit corresponds to $\log g_{wd} = 8.37$ (a $0.86M_{\odot}$ WD) and the upper limit corresponds to $\log g_{wd} = 8.54$ (a $0.96M_{wd}$ WD), and we have assumed $i = 60$ degrees.

In the case of the WD plus belt the distance d is given in a way similar to the WD only case with

$$d = 1000(\text{pc}) \times (R_{wd}/R_{\odot})/\sqrt{S},$$

where we set $d=65 \text{ pc}$.

The best-fitting white dwarf plus accretion belt fit with fixed distance ($d=65\text{pc}$) and a free radius R_{wd} yielded $T_{wd} = 23,000\text{K}$, Si abundance = $2.0 \times \text{solar}$, C abundance = $0.2 \times \text{solar}$, $V_{rot} \sin i = 400\text{km s}^{-1}$, with a radius $R_{wd} = 0.0087R_{\odot}$, corresponding to a mass $M_{wd} = 0.96M_{\odot}$ or $\log g = 8.54$. The belt temperature was $T_{belt} = 48,000\text{K}$, with a velocity of $V_{belt} \sin i \approx 4,000\text{km s}^{-1}$. In this model, the white dwarf contributed 83% of the FUV flux and the accretion belt 17% of the FUV flux, and the fractional area of the accretion belt was 2%. The χ^2_{ν} value of this fit was 7.06. This best-fitting white dwarf plus accretion belt

composite model is displayed in figure 5 and in Table 2 (model 12). We find this composite fit to be clearly superior to the single temperature and accretion disk - only fits. The remarkable lowering of the reduced χ^2_ν value for the accretion belt fit is additional confirmation of the findings by Sion et al. (1996, 1997, 2001) and Gänsicke & Beuermann (1996) that VW Hyi’s white dwarf has an inhomogeneous temperature distribution and that the most likely explanation is that of an accretion belt of higher temperature at its equatorial latitudes.

On the other hand, the best-fitting combination WD plus accretion belt model with a fixed WD radius and distance (model 13 in Table 2, $M = 0.86M_\odot$), had a $\chi^2_\nu = 10.9$. The stellar and belt parameters corresponding to this best-fit are as follows. The WD has an average surface temperature $T_{eff} = 22,000\text{K}$, $V_{rot} \sin i = 400\text{km s}^{-1}$, with solar abundances. The accretion belt has the parameters $T_{belt} = 50,000\text{K}$, and $V_{belt} \sin i = 3,000\text{km s}^{-1}$. The belt area is 2% of the WD surface and the belt contributes 23% of the total flux while the WD contributes 77% of flux. This composite two-temperature fit is shown in figure 6.

It is interesting to note that irrespective of whether the radius (and consequently the mass) of the white dwarf was kept fixed or not in the models, the best fit models with a lower χ^2_ν and with parameters (M_{wd} , d , i) consistent with the values assessed for the system were obtained for the WD plus belt composite model (models 12 & 13). The reason the fit is better is that the belt, with its high temperature, accounts for the flux shortward of 950 Å (where the WD does not contribute), and its high rotational velocity matches better the rather featureless spectrum of the second component. Model 10 (WD plus disk) has a $\chi^2_\nu \approx 11$, however its WD mass is too large $M_{wd} = 1.21$ and the inclination is too high at $i = 81$ degrees, therefore it can be ruled out. However, its relatively low χ^2_ν might be due to the fact that the hot inner disk is the main component in the FUV with (Table 2 in Wade & Hubeny (1998)) a rotational velocity $V_{rot} \sin i \approx 5,000\text{km s}^{-1}$ and a peak temperature $T_{max} \approx 30,000\text{K}$.

4. Discussion and Conclusion

The main observational result in this work is the confirmation that the *FUSE* spectrum of VW Hyi in quiescence cannot be modeled as a single WD temperature, and that at least two components are needed in the modeling of the data. The dominant component is that of a 23,000K WD, while the second component is some kind of true featureless continuum with a color temperature that is higher than that of the WD. It is possible that the two components exist only in the modeling of the FUV data and not in VW Hyi itself, for example if the WD is not heated homogeneously then we would have one component with a continuous range of temperatures that contribute to the spectrum.

4.1. The Cooling of the WD

VW Hyi has been previously observed mainly during quiescence, following normal (3 days) outburst and superoutburst (about 2 weeks). From an IUE archival study, Gänsicke & Beuermann (1996) assessed that the WD cools down exponentially to a mean temperature $T_{wd} \approx 19,000K$, with an exponential decay time of ≈ 3 days after normal outburst and ≈ 10 days after superoutburst. From this archival data alone it appears that the maximum temperature the WD reaches is about 23,000K, just after the end of a normal outburst and about 26,000K just after the end of a superoutburst. In Table 3 we recapitulate the recent observations of VW Hyi with different instruments. Most of the temperature estimates for the accreting WD are in the range described in Gänsicke & Beuermann (1996).

In the present work, the best fitting model to the *FUSE* data is a combination of a WD plus an accretion belt, which is noticeably better than the WD alone or the disk models. These two components to the spectrum of VW Hyi in quiescence help to resolve some of the differences in interpretation of UV spectra of VW Hyi in quiescence. The first component has a photospheric temperature of 23,000K, a rotation rate of 400 km s⁻¹ and chemical abundances that are reasonably consistent with previous HST FOS, GHRS and STIS results. This seems to indicate a cooling of the WD 11 days after a normal 3 day outburst. The second component has an effective temperature higher than that of the WD, and a featureless (rather flat) spectrum.

4.2. The Nature of the Second Component

Our numerical modeling is unable to account in detail for some of the features such as: (1) large discrepancies between our theoretical spectrum and the present *FUSE* data around 925 Å and 1100 Å; (2) the accretion belt model does not account for the upturn in flux at the Lyman limit, where the variability is strongest, which is also the region of the spectrum where the WD does not contribute to the flux, and consequently, neither the WD nor the accretion belt model can possibly be the source of the variability; (3) the OVI emission lines in the *FUSE* spectrum indicate the possible presence of an optically thin source in the system.

Therefore, the exact nature of the second component is still relatively uncertain, due to the lack of better models for spectra of the inner disk in a quiescent dwarf nova. As we mentioned in §1 the possible candidates for a second component are:

(1) an accretion belt, i.e. a fast rotating heated layer of the surface of the WD, possibly created in the outburst and which remains hot primarily because of the effective viscosity of

the WD.

(2) the boundary layer, i.e. the region between the inner edge of the disk and the stellar surface where the remaining kinetic energy of the accreting flow is released. This optically thin region reflects the instantaneous accretion rate and is expected to emit X-ray.

(3) an optically thick disk, however physically unjustified in the accretion disk limit cycle model (Cannizzo 1993), is what we are numerically able to model.

(4) or a corona/chromosphere above a cool disk.

At the present time, only the optically thick accretion belt and accretion disk can be numerically modeled, while no detailed modeling exists for the optically thin components (spectra). The results we obtained here indicate that the fast rotating belt is the best candidate for the source of the second FUV component.

4.3. The Accretion Belt

While the accretion belt model has improved the fits in VW Hyi in many observations (Sion et al. 2001), its existence has not yet been established. At some point, it was suggested [see e.g. (Huang et al. 1996a)] that the second hot component might actually be a hot ring near the inner edge of the disk. Huang et al. (1996a) identified the hot ring component as the “hot state” suggested in the accretion disk limit cycle model (Cannizzo 1993). In that theory, the outburst is triggered near the inner edge of the disk, and a heating front propagates to the outer edge, transforming the entire disk to the hot state. The quiescent state is achieved when a cooling front propagates back to smaller radii and shuts off the flow onto the WD. In that particular case, one expects the characteristics of the second component (observed in quiescence) to change rapidly in time, as the front moves inward through the disk. Recent observations (Sion et al. 2001), however, show that the second component in HST/STIS spectra of VW Hyi, taken 5 days apart, remains pretty much the same, making the scenario of the ring unlikely.

While accretion belts were first discussed theoretically by (Kippenhahn & Thomas 1978; Kutter & Sparks 1987, 1989), the first observational detection was for U Gem’s WD during quiescence (Long et al. 1993) based on *HUT* observations followed VW Hyi’s WD by Sion et al. (1996) using HST and Gänsicke & Beuermann (1996) using IUE archival spectra. The physical basis for an accretion belt is the tangential accretion of disk matter at the stellar equator with spin-up of the surface layers of the WD as it shears into the WD envelope with the slow conversion of kinetic energy to heat as a result of viscous heating in the differentially rotating atmosphere.

We have confirmed that the modeling of the *FUSE* spectrum of VW Hyi in quiescence

requires at least two components, as had been suggested by the earlier HST and HUT observations. The main component in the modeling is identified as the photosphere of a WD with a temperature of about 23,000K. The second component is a continuum relatively featureless with an effective temperature $\approx 48,000\text{K}$.

This discussion mainly serves to emphasize how far we are from an understanding of VW Hyi without a knowledge of the location of the emitting regions within the system. There could be a continuous range of temperatures, along with ranges in emitting areas and velocities, that contribute to the observed FUV spectrum. The only firm result that has been obtained here is that the second modeling component is fairly flat, and one possibility to produce such a flat component is with a high rotational velocity and a high temperature.

This work was supported by a Cycle 2 NASA *FUSE* grant to Villanova University.

REFERENCES

- Belloni, T. et al., 1991, A&A, 246, L44
- Cannizzo, J.K. 1993, ApJ, 419, 318
- Gänsicke, B.T., & Beuermann, K. 1996, A&A, 309, L47
- Gänsicke B.T. 1999, Tromsø, Norway White Dwarf Workshop, eds. J. Solheim & E. Meistas, ASP Conf. Ser.
- Hack, M., la Dous, C. 1993, Cataclysmic Variables and Related Objects, Monograph series on nonthermal phenomena in stellar atmospheres. NASA SP-507. Washington
- Huang, M., Sion, E.M., Hubeny, I., Cheng, F., & Szkody, P. 1996, ApJ, 458, 355
- Huang, M., Sion, E.M., Hubeny, I., Cheng, F.-H., & Szkody, P. 1996, AJ, 111, 2386
- Hubeny, I. 1988, Comput. Phys. Comm., 52, 103
- Hubeny, I., Lanz, T., & Jeffrey, S. 1994, Newsletter on Analysis of Astronomical Spectra (St. Andrews Univ.), 20, 30
- Hubeny, I., & Lanz, T. 1995, ApJ, 439, 875
- Kippenhahn, R., & Thomas, R.N. 1978, A&A, 63, 265
- Ko, Y.K., & Kallman, T.R. 1989, BAAS, 21, 1208
- Ko, Y.K., & Kallman, T.R. 1992, BAAS, 24, 1258
- Ko, Y.K., Lee, Y.P., Schlegel, E.M., & Kallman, T.R. 1996, ApJ, 457, 363
- Kutter, G.S., & Sparks, W.M. 1987, ApJ, 321, 386
- Kutter, G.S., & Sparks, W.M. 1989, ApJ, 340, 985
- La Dous, C., Meyer, F., & Meyer-Hofmeister, E. 1997, A&A, 321, 213L
- Liu, B.F., Meyer, F., & Meyer-Hofmeister, E. 1997, A&A, 328, 247L
- Long, K.S., Blair, W.P., Bowers, C.W., Davidsen, A.F., Kriss, G.A., Sion, E.M. & Hubeny, I. 1993, ApJ, 405, 327
- Long, K.S., Blair, W., Hubeny, I., & Raymond, J. 1996, ApJ, 468, 871

- Mateo, M., & Szkody, P. 1984, *AJ*, 89, 863
- Mauche, C., Wade, R.A, Polidan, R.S., van der Woerd, H., & Paerels, F.B.S. 1991, *ApJ*, 372, 659
- Mauche, C.W. 1996, in A. Evans and J.H. Woods (eds.), *Cataclysmic Variables and Related Objects*, 243 (Kluwer Academic Publishers, The Netherlands)
- Meyer, F., & Meyer-Hofmeister, E. 1989, *Astron.Gesellschaft Abstract Ser.*, 3, 64
- Moos, H.W. et al. 2000, *ApJ*, 538, L1
- Polidan, R.S., Mauche, C.W., & Wade, R.A. 1990, *ApJ*, 356, 211
- Sahnow, D.J. et al. 2000, *ApJ*, 538, L7
- Schoembs, R., & Vogt, N. 1981, *A&A*, 97, 185
- Sion, E. M. 1999, *PASP*, 111, 532
- Sion, E.M., Cheng, F., Long, K.S., Szkody, P., Huang, M., Gilliland, R., & Hubeny, I. 1995, *ApJ*, 439, 957
- Sion, E.M., Cheng, F.H., Huang, M., Hubeny, I., & Szkody, P. 1996, *ApJ*, 471, L41
- Sion, E.M., Cheng, F.H., Sparks, W.M., Szkody, P., Huang, M., & Hubeny, I. 1997, *ApJ*, 480, L17
- Sion, E.M., Cheng, F., Szkody, P., Gänsicke, B., Sparks, W.M., & Hubeny, I. 2001, *ApJ*, 561, L127
- Wade, R.A., & Hubeny, I. 1998, *ApJ*, 509, 350
- Wade, R.A., Hubeny, I., & Polidan, R.S. 1994, in "Interacting Binary Stars", ed.A. Shafter, *ASP Conf.Ser.* 56, 319 (San Fransisco: ASP)
- Warner, B. 1987, *MNRAS*, 227, 23

Figures Caption

Figure 1: *FUSE* spectrum of VW Hyi with lines identified. The sharp emission lines are not intrinsic to the source, they are due to air glow.

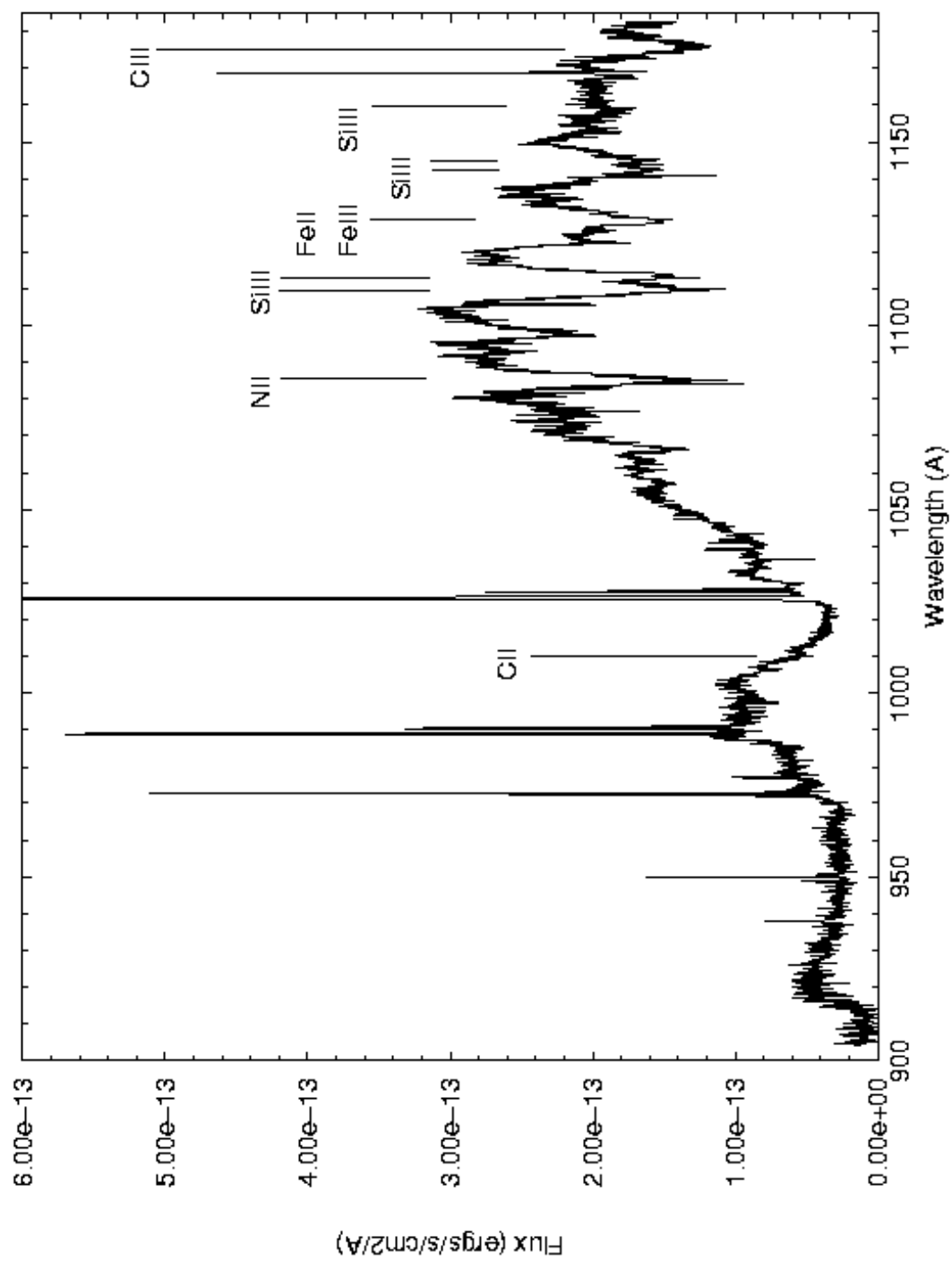
Figure 2: *FUSE* spectrum of VW Hyi together with the synthetic spectrum for a single white dwarf model with $T=26,000\text{K}$, $V_{rot} \sin i = 400\text{km s}^{-1}$, and the composition as specified in the text (model 1 in Table 2).

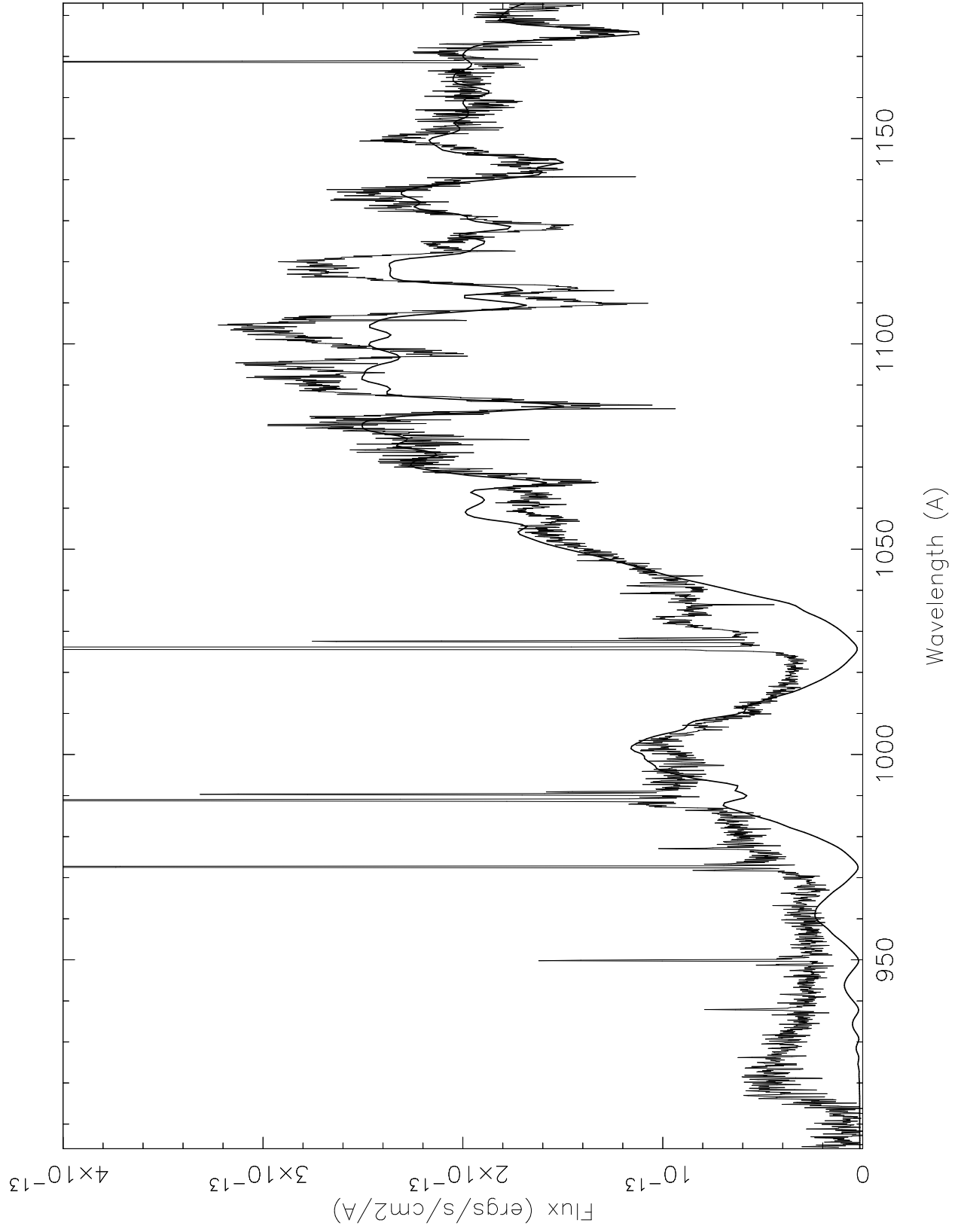
Figure 3: *FUSE* spectrum of VW Hyi together with the synthetic spectrum for an accretion disk model with a $1.03M_{\odot}$ central star, $\dot{M} = 1.0 \times 10^{-10.5} M_{\odot}\text{yr}^{-1}$, and a disk inclination of 81 degrees (model 6 in Table 2).

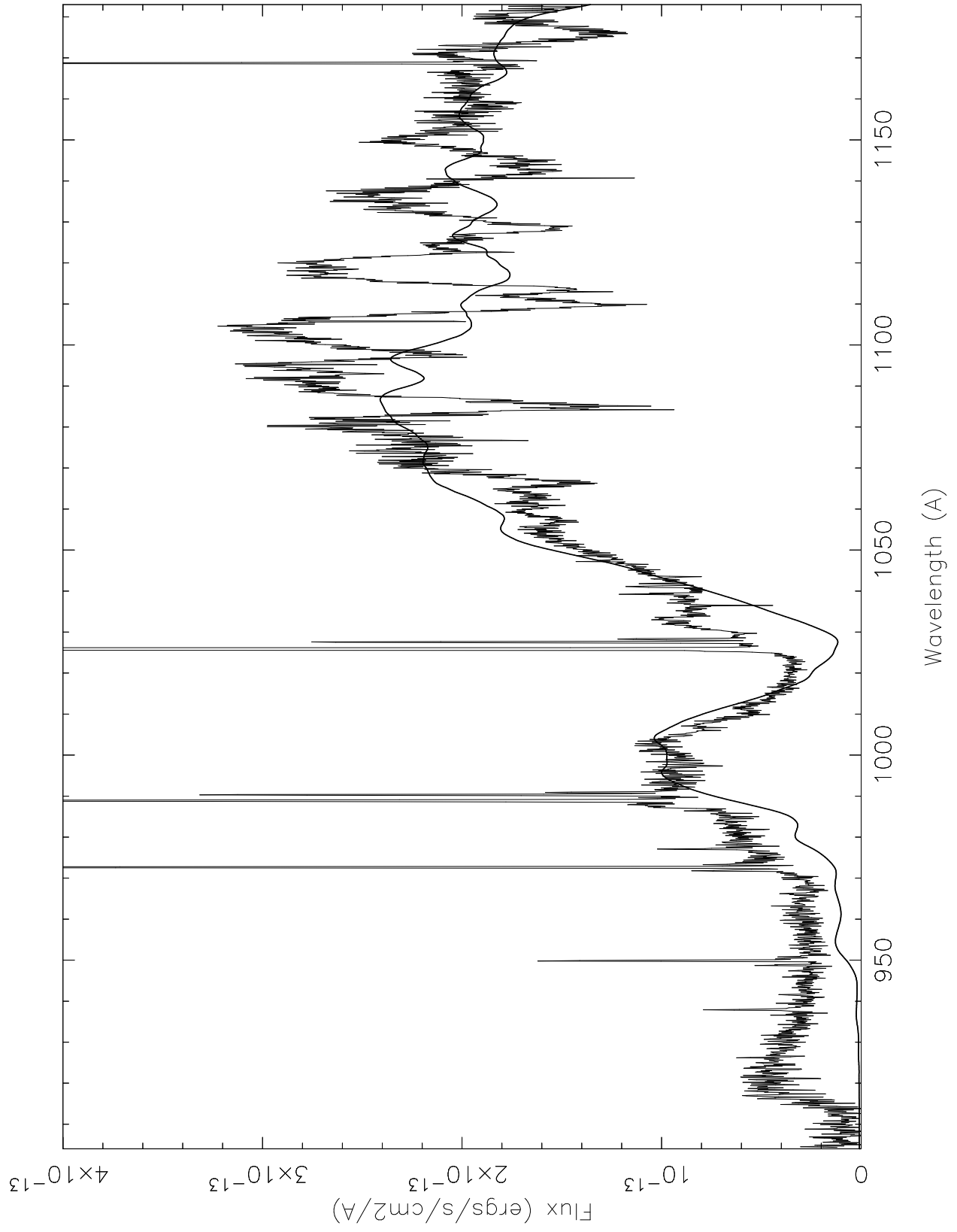
Figure 4: *FUSE* spectrum of VW Hyi together with the synthetic spectrum for a composite model fit consisting of a WD (dotted line) and an accretion disk (dashed line). The WD model has $T_{eff} = 23,000\text{K}$, $V_{rot} \sin i = 400\text{km s}^{-1}$ and the disk has an accretion rate of $3.16 \times 10^{-11} M_{\odot}\text{yr}^{-1}$ and an inclination of 81 degrees. The combination fit is shown with the solid line. (model 10 in Table 2)

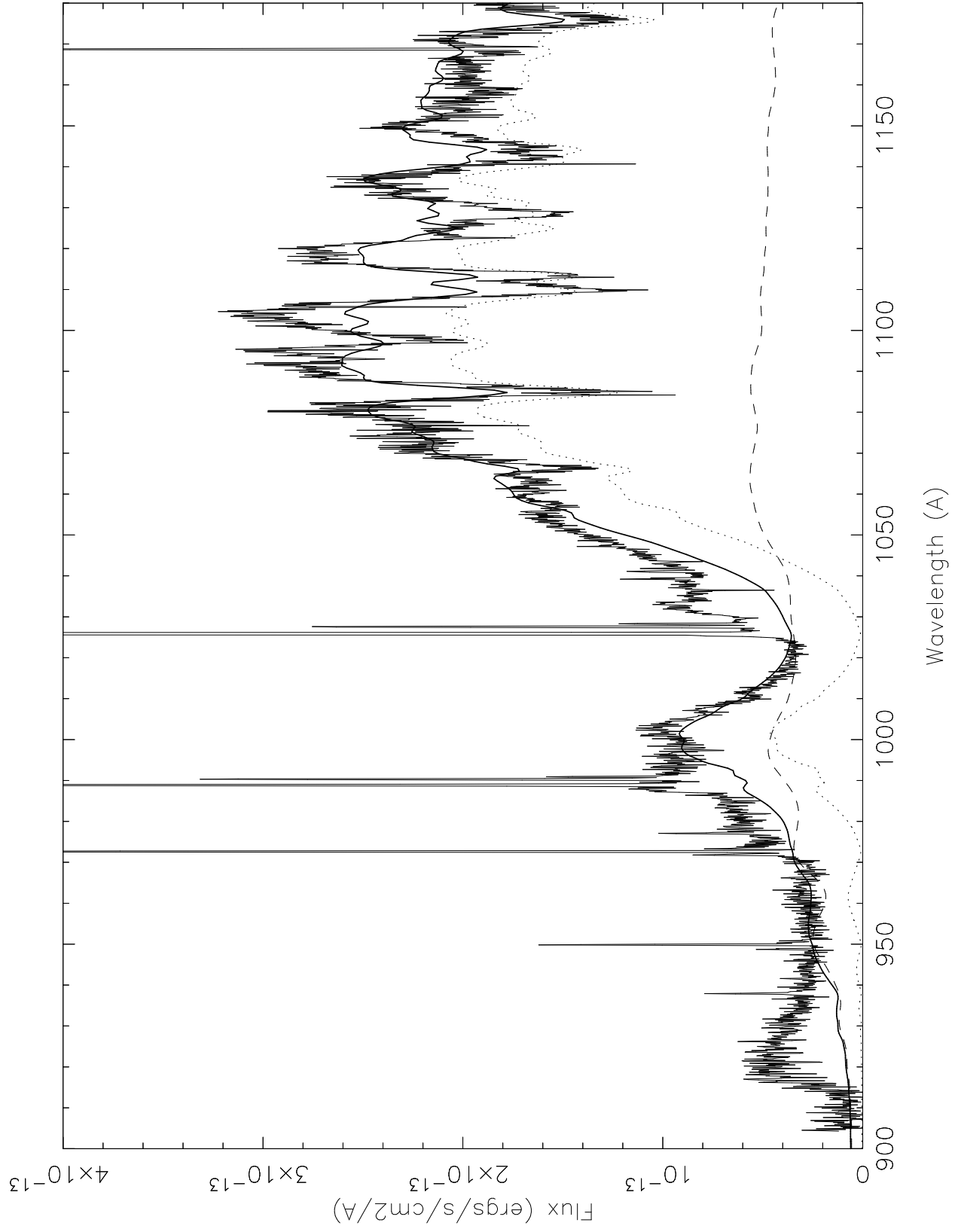
Figure 5: *FUSE* spectrum of VW Hyi together with the synthetic spectrum for a composite model fit consisting of a WD and an accretion belt. The white dwarf model has $M_{wd} = 0.96M_{\odot}$, $T=23,000\text{K}$, $V_{rot} \sin i = 400\text{km s}^{-1}$, and the composition as specified in the text, together with an accretion belt with $T = 48,000\text{K}$, and $V_{belt} \sin i = 4,000\text{km s}^{-1}$. The white dwarf photosphere flux is shown with the dotted line, the accretion belt flux is shown with the dashed line and their combined flux is shown with the solid line. (model 12 in Table 2)

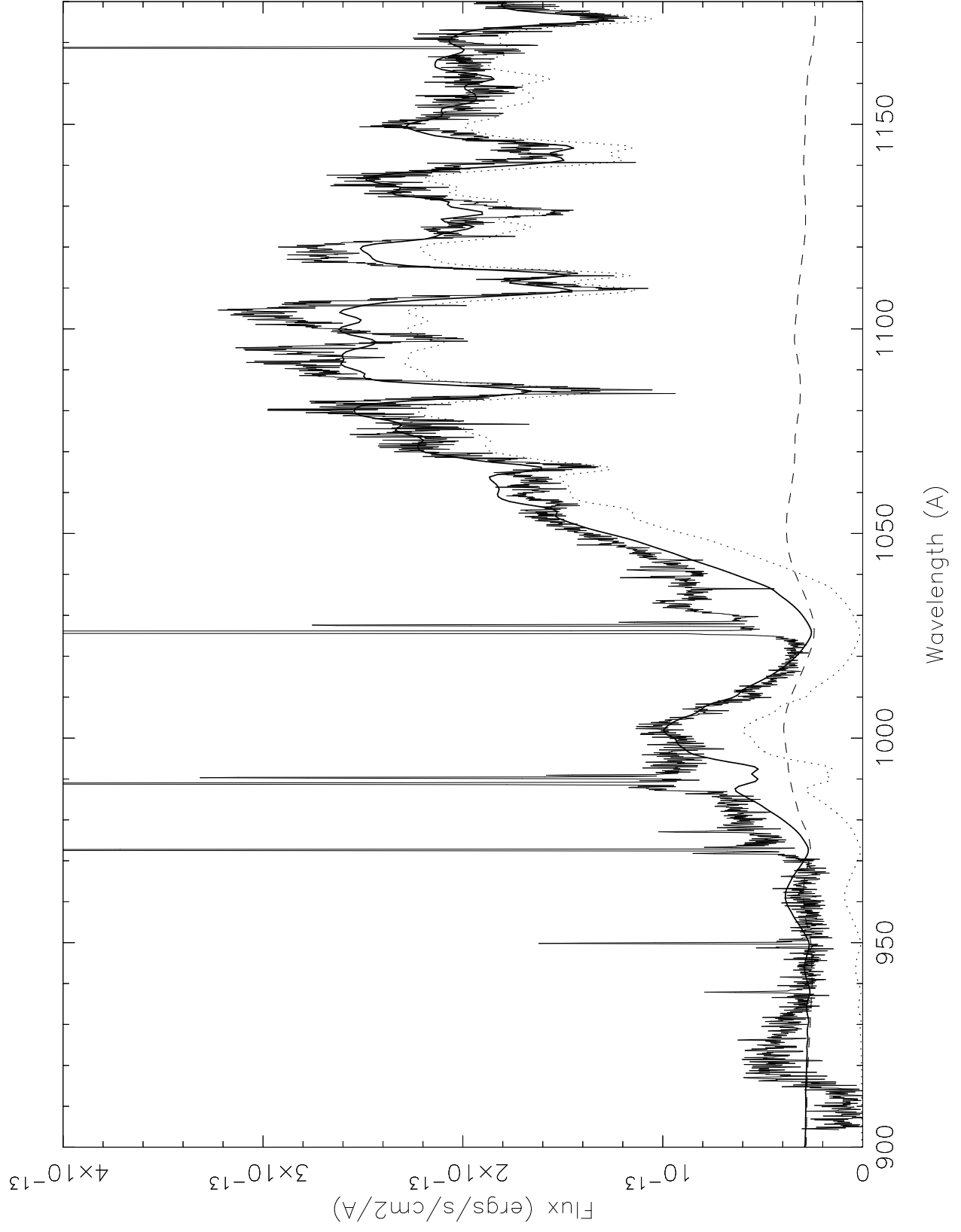
Figure 6: *FUSE* spectrum of VW Hyi together with the synthetic spectrum for a composite model fit consisting of a WD and an accretion belt. The white dwarf model has $M_{wd} = 0.86M_{\odot}$, $T=22,000\text{K}$, $V_{rot} \sin i = 400\text{km s}^{-1}$, and solar composition, together with an accretion belt with $T = 50,000\text{K}$, and $V_{belt} \sin i = 3,000\text{km s}^{-1}$. The white dwarf photosphere flux is shown with the dotted line, the accretion belt flux is shown with the dashed line and their combined flux is shown with the solid line. (model 13 in Table 2)











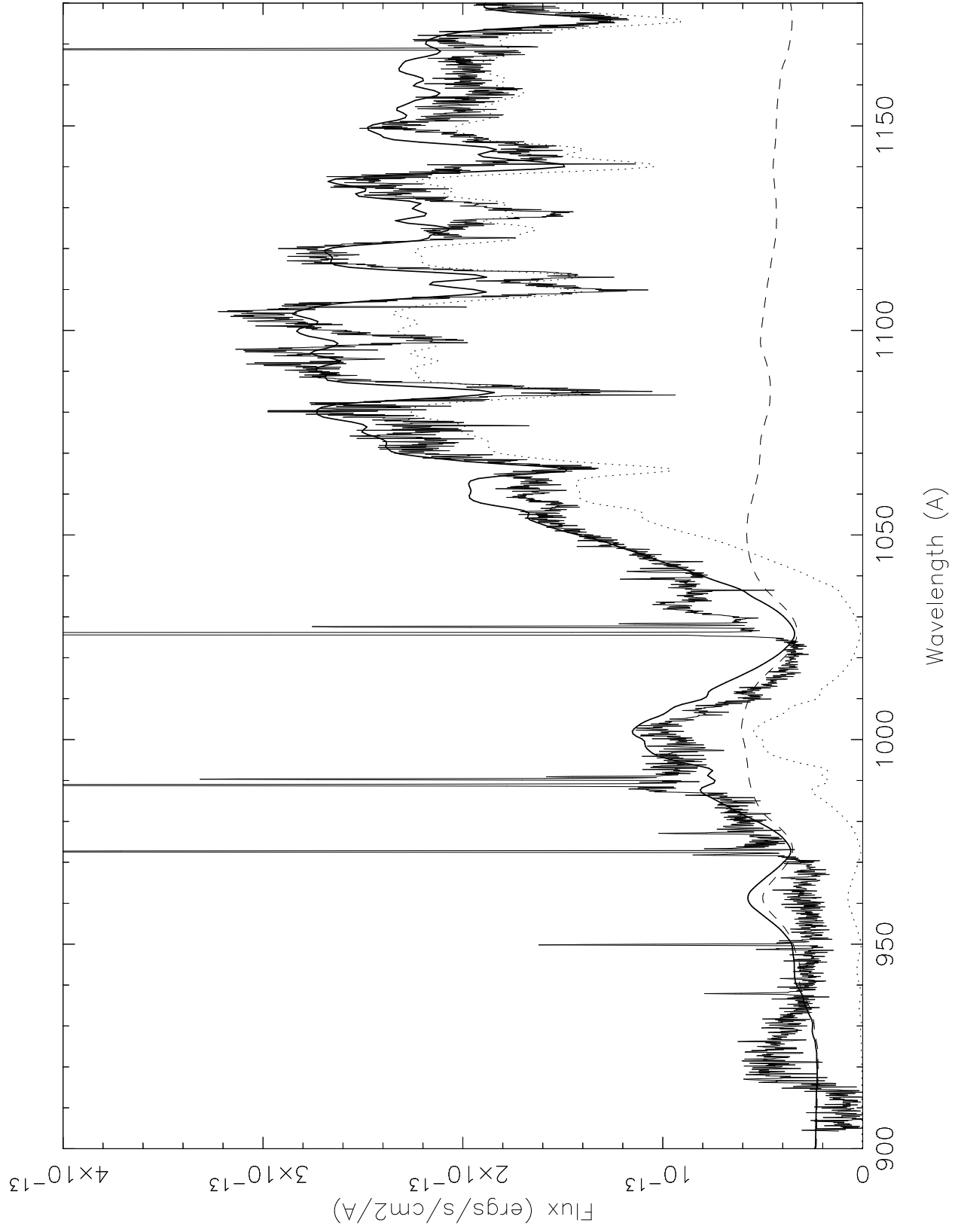


Table 1. Line identification for the *FUSE* spectrum of VW Hyi

λ Å	EQW ¹ Å	FWHM ² Å	Line	Wavelength Å
1085.11	2.064	3.675	N II	1085.7
1112.04	4.234	7.214	Si III	1113.2
1128.13	3.488	9.144	Fe III	1128.7
			Fe II	1129.2
1143.68	2.931	8.052	Si III	1144.3
1159.08	2.409	13.84	Si III	1160.2
1175.11	1.806	4.596	C III	1174.9
				1175.3
				1175.6
				1175.7
				1176.0
				1176.4

¹In the second column: EQW is the line equivalent width in Å.

²In the third column: FWHM is the full width at half maximum in Å.

Table 2. Best fit models for VW Hyi

model	n	χ^2_ν	T_{wd} 1000K	log g cm/s ²	$V_{rot} \sin i$ km/s	Si ☉	C ☉	M_{wd} M_\odot	Log \dot{M} $M_\odot \text{yr}^{-1}$	i deg	T_{belt} 1000K
WD	1	14.8	26	8.80	400	0.5	0.1	1.14			
WD	2	32.0	22	8.37	400	1.0	1.0	0.86			
WD	3	28.2	23	8.37	400	1.0	1.0	0.86			
WD	4	81.5	24	8.37	400	1.0	1.0	0.86			
WD	5	226.3	25	8.37	400	1.0	1.0	0.86			
disk	6	19.9						1.03	-10.5	60	
disk	7	10 ⁴						0.80	-9.5	60	
disk	8	29.8						0.80	-10	60	
disk	9	286						0.80	-10.5	60	
WD+disk	10	11.0	23	8.99	400	0.5	0.1	1.21	-10.5	81	
WD+disk	11	32.9	21	8.23	400	1.0	1.0	0.80	-10.5	60	
WD+belt	12	7.06	23	8.54	400	2.0	0.2	0.96			48
WD+belt	13	10.9	22	8.37	400	1.0	1.0	0.86			50

Table 3. Some Recent Observations of VW Hyi

Instrument	T_{eff} 1000K	\dot{M} M_{\odot}/yr	Type ¹	Days ²	Reference
IUE	18.0	1×10^{-10}		Q	Wade et al. 1994
HST/FOS	22.5		NO	1-Q	Sion et al. 1996
HST/FOS		3×10^{-9}	SO	5-O	Huang al. 1996
HST/FOS	20.5		SO	10-Q	Sion et al. 1996
HUT	18.7	4×10^{-11}	NO	13-Q	Long et al. 1996
HST/GHRS	22.0		NO	30-Q	Sion et al. 1997
HST/STIS	22.5		SO	2-Q	Sion et al. 2001
HST/STIS	21.5		SO	7-Q	Sion et al. 2001
FUSE	23.0		NO	11-Q	this work

¹In the fourth column: NO - Normal Outburst; SO - Superoutburst.

²In the fifth column: The number indicates how many days the observation was made into Q - quiescence or O - outburst.